Stability Analysis of Variable Geometry Helicopters

Rahul Ramanujam
Project Associate
rahuliitk12@gmail.com

Shyamal Rao
Graduate Student
shyamalrao@gmail.com

Abhishek
Assistant Professor
abhish@iitk.ac.in

Department of Aerospace Engineering
Indian Institute of Technology Kanpur
Kanpur, India

ABSTRACT

This paper discusses the effect of variation of rotor blade radius and chord on the stability characteristic of a variable geometry helicopter. The current mathematical model synthesizes the rigid fuselage motion model with 6 degrees of freedom, coupled with flap only rigid rotor blade motion model and a quasi-steady aerodynamics model equipped with non-uniform Drees inflow model. The baseline correlation study is based on the DLR research Bo105-S123 helicopter data. The trim and stability results of the proposed model is validated with results available in literature. The stability of the helicopter is investigated by increasing the main rotor blade radius by 5% and 10%. Similar study is done on the chord by increasing it by 10% and 20%. A new coupled pitch oscillatory mode is observed when the blade radius and chord is increased from its baseline by the combination of pitch mode-1 and pitch mode-2.

NOTATIONS

c	*main rotor blade chord, (m)*
$c110$	*main rotor blade chord incremented by 10%, (m)*
$c120$	*main rotor blade chord incremented by 20%, (m)*
C_T	*main rotor thrust coefficient*
g	*acceleration due to gravity, (m/s^2)*
I_x, I_y, I_z	*moments of inertia about the fuselage x-, y- and z-axes, $(kg\,m^2)$*
I_{xz}	*product of inertia about the fuselage x- and z-axes, $(kg\,m^2)$*
K_x, K_y	*weighting factors and represent the deviation of the inflow from the uniform value predicted by momentum theory*
L, M, N	*external aerodynamic moments about the x-, y- and z-axes, (Nm)*
M_a	*mass of helicopter, (kg)*
p, q, r	*fuselage rotational velocity components along x-,y- and z-axes, (rad/s)*
R	*main rotor blade radius, (m)*
$R105$	*main rotor blade radius incremented by 5%, (m)*
$R110$	*main rotor blade radius incremented by 10%, (m)*
u, v, w	*fuselage translational velocity components along x-,y- and z-axes, (m/s)*
X, Y, Z	*external aerodynamic forces acting along the x-, y- and z-axes, (N)*
α	*fuselage pitch attitude, (rad)*
λ_o	*non-dimensional mean induced velocity*
λ_i	*non-dimensional induced velocity*
χ	*main rotor wake skew angle, (rad)*
μ	*advance ratio*
μ_x, μ_z	*advance ratio defined parallel and perpendicular to the rotor disk*
θ_o, θ_{tr}	*main and tail rotor collective pitch angles, (rad)*
θ_{1c}, θ_{1s}	*longitudinal and lateral cyclic pitch, (rad)*
τ	*real part of eigenvalue or damping, (rad/s)*
ω	*imaginary part of eigenvalue or damped natural frequency, $(1/s)$*
ψ_k	*rotor blade azimuth angle, (rad)*
ϕ	*fuselage roll attitude, (rad)*

INTRODUCTION

Designing a multi-role helicopter which can adapt to wide range of missions, e.g. be able to efficiently hover for long periods of time as well as cruise efficiently at very high speeds, is a designer's nightmare. No single fixed design can meet such stringent set of requirements. Variable speed and variable geometry rotors offer the possibility of development of such mission adaptive helicopters. Historically, the development of helicopter was hampered during its early years of evolution because of the lack of understanding of stability parameters and therefore adequate control over the vehicle was difficult to achieve. Preliminary knowledge of stability and

Presented at the 4th Asian/Australian Rotorcraft Forum, IISc, India, November 16–18, 2015.

control is essential for the design of the helicopter with desirable response. Stability is the tendency of any object to show the tendency to return towards equilibrium state after getting disturbed. Stability is essential to ensure safe operation of helicopters and access the aspect of handling quality. However, an unstable system is preferred by the pilots during combat maneuvers, as lack of stability implies higher maneuverability.

The concept of in-flight variation of blade/wing geometry is commonly referred to as morphing blade/wing technology. Its potential uses include wide areas such as wind turbines, aircrafts, helicopters and unmanned aerial vehicles. Variable geometry blade concepts has been under investigation since 1973 when Fradenburgh et al. (Ref. 1) investigated the performance benefits of a telescoping-blade rotor system (TRAC). In 1994 Matuska et al. (Ref. 2) worked on Variable diameter rotor and gave a detailed explanation of the mechanism involved in it. Similar morphing concepts such as trailing-edge flap control, spoiler flap, inflatable camber, active blade twist etc. were also implemented in wind turbines for performance benefits, see Refs. 3, 4. In recent years, various active and passive means of rotor blade morphing has been investigated by various researchers. Most of these studies have dealt with the physical methodology of achieving blade morphing and / or studied the effect of variable geometry on the performance characteristics of the helicopter, as discussed below.

Moser et al. studied the chord morphing over a spanwise section of blades and observed that it can alleviate stall and improve the rotorcraft performance when flying close to the flight envelope boundaries(Refs. 5). In a similar study by Khoshlahjeh et al. it was concluded that 20% increase in chord length has a considerable reduction in the power consumption at the stall region (Refs. 6). A study done by Kang et al. showed that a combination of variable chord and variable rotor speed was effective approach for improving the aircraft maximum forward speed while keeping the required power at minimal (Refs. 7). Another computational study of significance for variable radius and variable RPM rotors was carried out by Mistry et al. (Ref. 8). They showed a maximum power reduction of 14% in cruise (80–100 kt) with RPM variation alone. Up to 20% reduction in power was achieved by radius variation for high-and-heavy flight conditions. Combination of variable radius and RPM resulted in higher overall reduction in power than the use of RPM or radius variation alone. These studies focused on performance enhancement due to morphing of the main rotor blade, the effect of morphing rotor concept on the stability characteristic of the helicopter has not yet been fully understood.

The aim of the present work is to study the impact of variable geometry on the stability modes of the helicopter. For this, a baseline flight dynamics analysis is developed and validated using available data in literature. A rigid blade model having only flap degree of freedom is coupled to a quasi-steady aerodynamics model to perform stability analysis. Drees model is used for inflow calculation. In the present analysis, the effect of rotor blade geometry on the eigenvalues is systematically studied. Eigenvalues associated with the system matrix for steady forward flight speeds from hover to 235 km/hr are computed and their variation with blade radius and chord is analyzed.

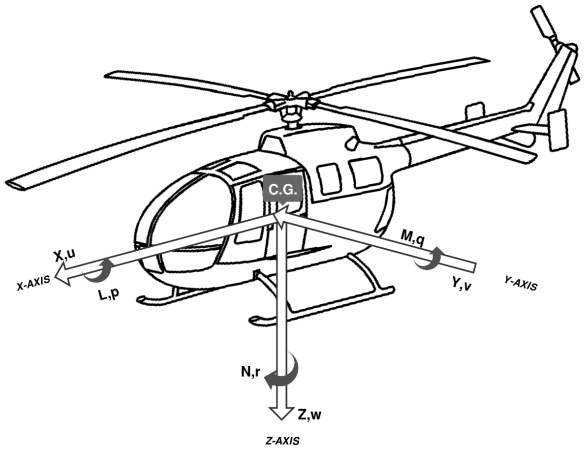

Fig. 1. Body fixed coordinate system used for present analysis

METHODOLOGY

The aerodynamic loading (forces and moments) due to rotor blades is estimated using Blade Element Theory. Blade has flap and rotational degree of freedom. The flow velocities at each radial and azimuth location of the blade are determined from the transformation of velocities from non-rotating to rotating blade coordinates. The sectional lift, drag and moments are calculated using the flow velocities. The integrated sectional loads averaged for the number of blades over one revolution are then transferred to the c.g. of the helicopter. The centrifugal force created due to rotor blades contribute to the inertial loads. Similar to the calculation of aerodynamic loads due to rotor blades, the inertial loads involve the transfer of the mean inertial forces to the c.g. of the helicopter. Other loads include weight of the helicopter and the side force and moments due to tail rotor. Chord distribution along the radial direction is constant. The geometric blade angle consists components from linear blade twist, cyclic and collective.

Inflow Model

A simple first harmonic non-uniform inflow model developed by Glauert with further improvements done by Drees in 1949 (Ref. 9) is used to model the inflow variation. The model incorporates both radial and azimuth variation in the inflow as shown below:

$$\lambda_i = \lambda_o(1 + K_x r_k cos(\psi_k) + K_y r_k sin(\psi_k))$$

where the expression for the mean induced inflow based on momentum theory is

$$\lambda_o = \frac{C_T}{2\sqrt{\mu^2 + \lambda_o^2}}$$

and the inflow coefficients are expressed as

$$K_x = \frac{4}{3}(\frac{1-cos(\chi)-1.8\mu^2}{sin(\chi)}),\ K_y = -2\mu$$

and the wake skew angle is defined as

$$\chi = tan^{-1}(\frac{\mu_x}{\mu_z+\lambda_i})$$

Coordinate systems

The resultant forces and moments correspond to a system of body-fixed axes centered at the helicopter center of gravity (CG). The body-fixed coordinate system is fixed to the CG of the aircraft and its orientation changes with that of the helicopter. The corresponding components of the translational and rotational velocities are shown in Fig. 1.

Assumptions

The simplifying assumptions made in the development of the current flight dynamics analysis are listed below:

- The trim and stability analysis are associated with steady and level flight conditions.
- The rotor was assumed to be operating at constant rotational speed.
- It is assumed that the hub is rigid with no bending deflection at the pitch bearing, and the kinematic pitch-bending coupling is absent.
- The study is based on quasi-steady assumptions, which means that the changes in physical quantities occur instantaneously.
- Assumption is made that x-z plane is the plane of symmetry for the helicopter.
- Only blade flap degree of freedom is considered. Lead lag and torsional degrees of freedom are not modeled yet.
- Stall and compressibility effects are not taken into consideration.
- The assumptions made in the 6 DOF equilibrium equations are that the higher order rotor and inflow dynamics are much faster than fuselage motions and have adequate time to reach the steady state within the response modes of the helicopter.

Equation of Motion

The equations of motion governing the rigid body dynamics of helicopter in nonlinear form are given by

$$\dot{x} = F(x,U,t)$$

where, $\mathbf{x} = \{u,v,w,p,q,r,\theta,\phi\}$ is the helicopter state vector and $\mathbf{U} = \{\theta_o,\theta_{1s},\theta_{1c},\theta_{tr}$is the control vector. Equilibrium equations along with the Euler angles are given by the following expressions:

$$\begin{aligned}
\dot{u} &= -(wq-vr)+\frac{X}{M_a}-gsin\theta \\
\dot{v} &= -(ur-wp)+\frac{Y}{M_a}+gcos\theta sin\phi \\
\dot{w} &= -(vp-uq)+\frac{Z}{M_a}+gcos\theta cos\phi \\
I_x\dot{p} &= (I_y-I_z)qr+I_{xz}(\dot{r}+pq)+L \\
I_y\dot{q} &= (I_z-I_x)rp+I_{xz}(r^2-p^2)+M \\
I_z\dot{r} &= (I_x-I_y)pq+I_{xz}(\dot{p}-qr)+N
\end{aligned}$$

Kinematic equations are given by

$$\begin{aligned}
\dot{\phi} &= p+qsin\phi tan\theta+rcos\phi tan\theta \\
\dot{\theta} &= qcos\phi-rsin\phi
\end{aligned}$$

Based on small perturbation theory, any disturbed motion is described as a perturbation from the trim, written in the form

$$\mathbf{x} = \mathbf{x}_e+\delta\mathbf{x}$$

where $\mathbf{x}_e$ is the equilibrium value of the state vector and $\delta\mathbf{x}$ is the perturbation.The loads corresponding to disturbed motion states is given by

$$\begin{aligned}
\Pi &= \Pi_e+\delta\Pi \\
\delta\Pi &= \sum_{J=j_i}(\frac{\partial\Pi}{\partial J})\delta J
\end{aligned}$$

where

$$\begin{aligned}
j_i &= \{u,v,w,p,q,r,\theta_o,\theta_{1s},\theta_{1c},\theta_{tr}\} \\
\Pi &= \{X,Y,Z,L,M,N\}
\end{aligned}$$

The linearized equations of motion for the full 6 degree of freedom (DoF) system describing the perturbed motion about the trim condition is given in the form

$$\dot{x}-Ax = BU$$

Stability Analysis

The stability of the helicopter can be determined by the stability of individual modes. The stability of the individual modes can be determined by sign of the real part of the eigenvalues. A positive sign of the eigenvalue indicates stability and negative sign indicates instability. The illustration of eigenvalues of each mode in complex plane with forward speed can demonstrate the stability of the system at various speeds.

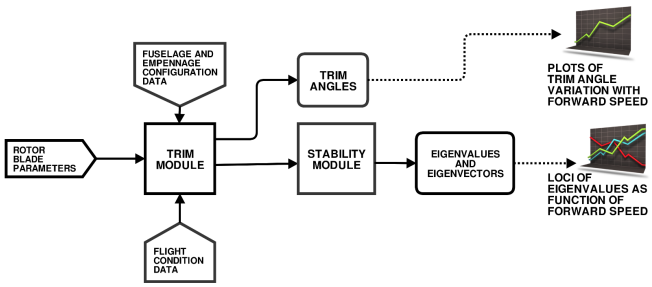

Fig. 2. Flow chart representing the computational analysis

This type of representation of eigenvalues is called as root locus plot. The motion of a helicopter can be described by the equation

$$\dot{x} - Ax = 0$$

The computed eigenvalues(λ) satisfy the equation

$$det[\lambda I - A] = 0$$

COMPUTATIONAL ANALYSIS

The overall program comprises of 3 modules interfaced to one another which are (1) aircraft input parameters module (2) trim module and (3) stability module.

The aircraft input parameters module consists of rotor blade parameters, fuselage and empennage configuration data and flight condition data. The data for BO 105 baseline configuration used for present analysis is listed in Table. 1. A general outline of the main features of the program is described in the Fig. 2.

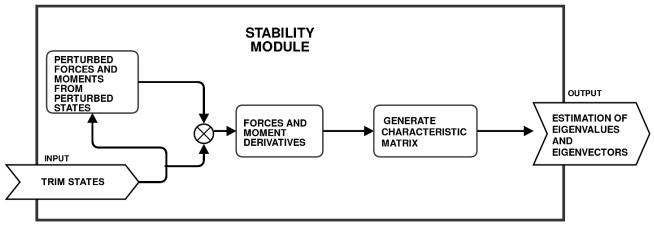

Fig. 3. Flow chart describing the functioning of stability module

Trim module accepts the blade parameters, fuselage and empennage configuration data and flight condition data as input and estimates the trim angles for hover and steady level flight conditions. The trim states are evaluated by solving the nonlinear equilibrium equations using Newton-Raphson method. The blade dynamics equation is solved using Newmark's algorithm, and all blade-loads and hub-loads are calculated by performing numerical integration over 20 blade segments using six point Gauss quadrature. This generalized numerical formulation makes the analysis modular for future refinements. Trim angles are recorded and their variation with respect to the advance ratio is visualized with the help of graphs.

The stability module estimates the eigenvalues and eigenvectors corresponding to each of the trim states by evaluating the force and moment derivatives required to generate the characteristic matrix. The stability derivatives are evaluated numerically with the help of first ordered finite difference method. Root locus graphs are plotted to visualize the degree of stability for each of the eigenvalues. The working of the stability module is elaborated in the Fig. 3.

Table 1. Baseline configuration data for Bo105

Mass and moments of Inertia	
Mass	2200 kg
I_x	1433 $kg\,m^2$
I_y	4973 $kg\,m^2$
I_z	4099 $kg\,m^2$
I_{xz}	660 $kg\,m^2$
Main rotor	
Radius	4.91 m
Blades	4
Chord	0.27 m
Profile	NACA 23012
Solidity	0.07
Tip sweep	0^o
Twist	-6.2^o
Shaft Angle	-3.0^o
Tail rotor	
Radius	0.95 m
Blades	2
Chord	0.179 m
Profile	NACA 0012
Solidity	0.12
Twist	0^o
Empennage	
Fin area	0.805 m^2
Tailplane area	0.803 m^2

RESULTS

The rotor performance code is validated using the flight test data and HELISIM results. The flight test data and HELISIM results are taken from (Ref. 10). The collective control angle is compared with flight test data in Fig. 4(a). Present analysis and HELISIM underpredict the collective angle. This is essentially because both the analyses did not model elastic twist deformation, which tends to decrease the sectional angle of attack due to nose-down elastic twist deformation, thereby increasing the required collective input. The lateral cyclic angle comparison is shown in Fig. 4(b). Present analysis underpredicts from low to moderate speed and overpredicts at high speed. The magnitude of longitudinal cyclic angle is overpredicted and follows the trend of the flight test data as seen in the Fig. 4(c). The present analysis follows the

Table 2. Comparison of Bo 105 eigenvalues

Mode of motion	AFDD	CERT	DLR	U.S Army	Helisim	Present model
	$[\varsigma,\omega_o]$	$[\varsigma,\omega_o]$	$[\varsigma,\omega_o]$	$[\varsigma,\omega_o]$	$[\varsigma,\omega_o]$	$[\varsigma,\omega_o]$
Phugoid oscillation	[-0.36, 0.30]	[-0.17, 0.32]	[-0.15, 0.33]	[-0.33, 0.32]	[-0.058, 0.3]	[-0.291, 0.30]
Dutch roll oscillation	[0.22, 2.60]	[0.13, 2.51]	[0.14, 2.50]	[0.19, 2.65]	[0.214, 2.64]	[0.153, 3.26]
	$(\frac{1}{T})$	$(\frac{1}{T})$	$(\frac{1}{T})$	$(\frac{1}{T})$	$(\frac{1}{T})$	$(\frac{1}{T})$
Roll mode	(8.32)	[0.99, 2.89]	(8.49)	(10.76)	(13.72)	(14.42)
Aperiodic pitch mode 1	(6.04)	—	(4.36)	(6.69)	(4.25)	(4.60)
Aperiodic pitch mode 2	(0.49)	(0.66)	(0.60)	(0.51)	(0.653)	(2.02)
Spiral mode	(0.03)	(-0.05)	(0.02)	(0.03)	(0.024)	(0.183)

Shorthand notation

$[\varsigma,\omega_o]$ implies $s^2+2\varsigma\omega_o+\omega_o^2$, ς = damping ratio, ω_o =undamped natural frequency (rad/sec)

$(1/T)$ implies $(s+1/T)$,(rad/sec)

trend observed for results predicted using HELISIM, however the magnitude of the cyclic angles is largely overpredicted by 0.5° to 1.0°. This difference may be due to the differences in inflow modelling. The HELISIM predictions have been obtained using dynamic inflow model. The tail rotor collective from the present analysis closely captures the flight test trend as shown in the Fig. 4(d). Pitch and roll attitudes are shown in the Figs. 4(e) and 4(f).

In the present analysis, two oscillatory modes and four non oscillatory modes are observed during forward flight for the baseline model. The non oscillatory modes are the aperiodic pitch mode 1, aperiodic pitch mode 2, roll mode and spiral mode. Longitudinal oscillatory mode is called the phugoid and the lateral oscillatory mode is called the dutch roll mode. The eigenvalues calculated for stability are validated using flight test data (obtained using system identification) and simulated results available in literature (Refs. 10–12) for the forward flight speed of 80 knots (148.16 km/hr) as shown in the Table 2. Present analysis shows fair correlation for non oscillatory modes and damping ratio and undamped natural frequency of oscillatory modes.

The loci of the dutch roll eigenvalue is shown in the Fig. 5(a). The stability of the dutch roll mode shows a steep increase with forward speed at low speeds. Further increase in forward speed shows a decreasing effect on dutch roll stability before increasing at higher speed. The frequency of the dutch roll shows a steady increases with forward speed. The loci of the phugoid mode is shown in the Fig. 5(c). The stability of the phugoid mode increases steadily with forward speed and it decreases after 56.68 km/hr. The frequency of the phugoid mode decreases with forward speed.

The loci of the aperiodic pitch mode-1 eigenvalue is shown in the Fig. 5(d). The stability of the pitch mode-1 increases up to 62.78 km/hr and then starts to decrease for further increase in forward speed. Fig. 5(b) shows decrease in stability up to a speed of 62.78 km/hr and then the stability increases for further increase in forward speed for aperiodic pitch mode-2. The roll stability increases with forward speed as shown in the Fig. 5(e). The loci of the spiral mode eigenvalues is shown in the Fig. 5(f). Spiral mode stability decreases with increase in forward speed.

The eigenvectors of the baseline model for all modes are shown in polar form in the Fig. 6 for the forward speed of 80 knots (148.16 km/hr). The eigenvectors are normalized such that its magnitude equals unity. Figure 6(a) shows the magnitude of the eigenvector components for dutch roll oscillation. Since the mode is oscillatory each component has magnitude and phase. The yaw rate (r), pitch rate (q) and roll angle (ϕ) are observed to have significant influence on dutch roll mode. Similarly eigenvector components of phugoid oscillation also has magnitude and phase as shown in the Fig. 6(b). Pitch angle (θ) and pitch rate (q) significantly contribute to the phugoid oscillation. Aperiodic pitch mode-1 and pitch mode-2 has considerable contribution from pitch rate (q) and yaw rate (r) as shown in the Figs. 6(c) and 6(d). Roll mode eigenvector is shown in the Fig. 6(e). The pitch rate(q) has an opposing effect to the roll rate (p) and yaw rat e(r) in the roll mode. Fig. 6(f) shows the eigenvector for spiral mode and it has pitch angle (θ) and roll angle (ϕ) as major contributors.

Effect of Variation of Rotor Radius

The schematic diagram of the radius extension, change in mass per unit length (mpl) and blade twist variation is shown in the Fig. 7. The blade geometry remains and sectional properties remain unchanged irrespective of the change in blade radius. Radius of the blade is increased by 5% and 10% of the baseline and its effect on stability modes are studied.

The roll mode variation due to radial change is shown in the Fig. 8(a). It is evident that the stability of the roll mode at lower speed decreases with increase in radius, however as the speed increases the effect of radius change on the roll mode decreases. The stability of the spiral mode slightly increases at higher speed and doesn't show any considerable increase at lower speeds.

The dutch roll oscillation variation with radius is shown in the Fig. 8(c). At lower speeds, baseline radius is slightly

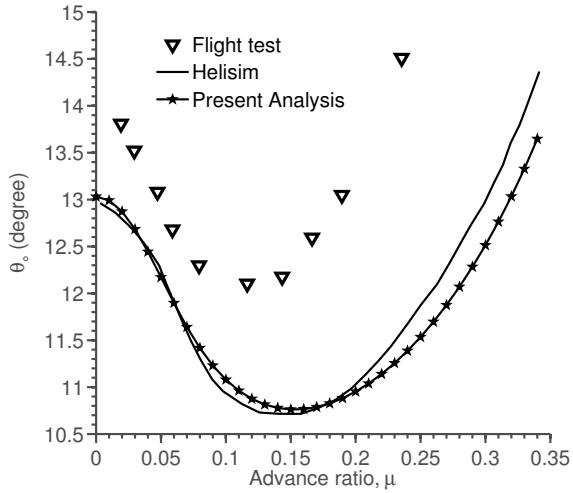

(a) Main rotor collective

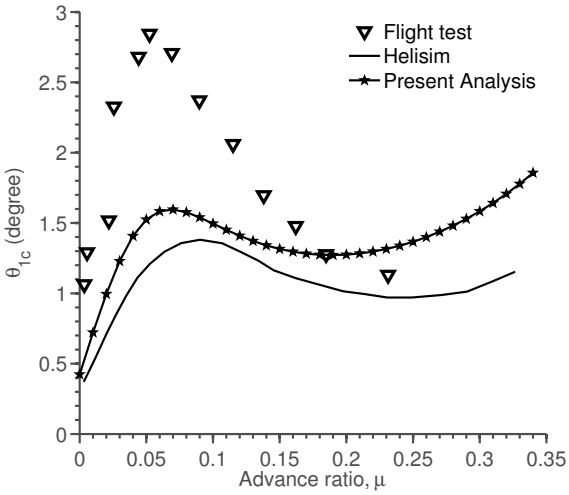

(b) Lateral cyclic

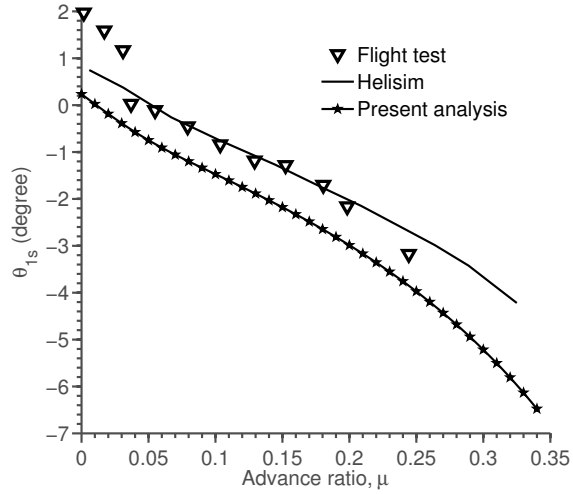

(c) Longitudinal cyclic

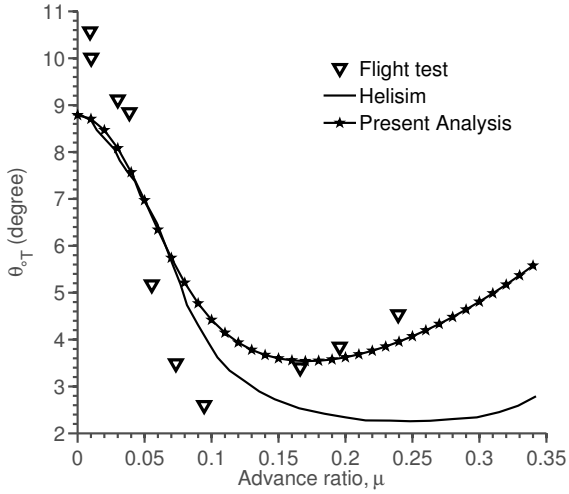

(d) Tail rotor collective

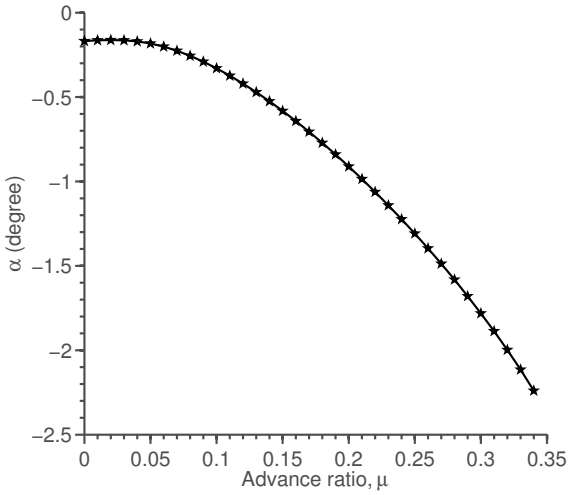

(e) Pitch attitude

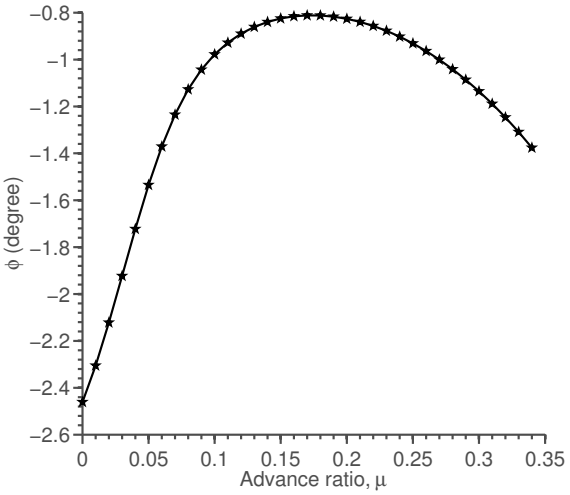

(f) Roll attitude

Fig. 4. BO 105 trim angles for forward speed at C_T =0.0049

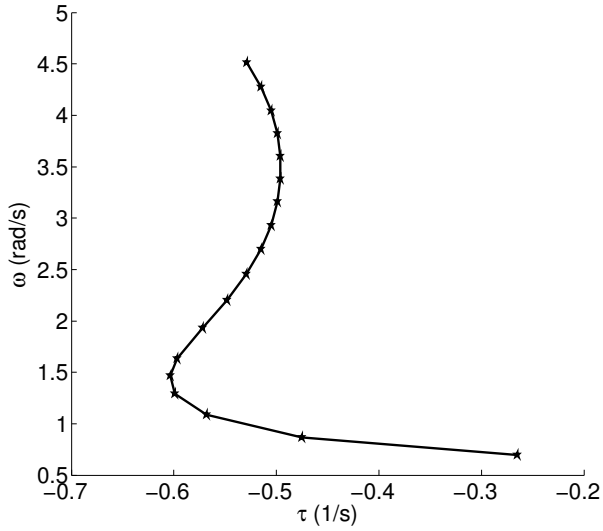

(a) Dutch roll oscillation

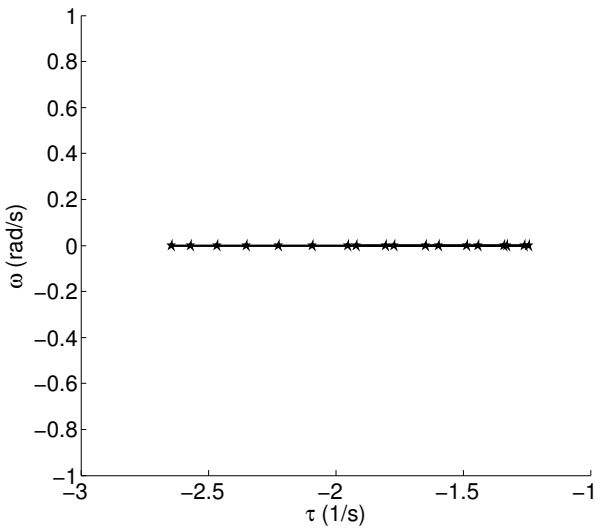

(b) Aperiodic pitch mode 2

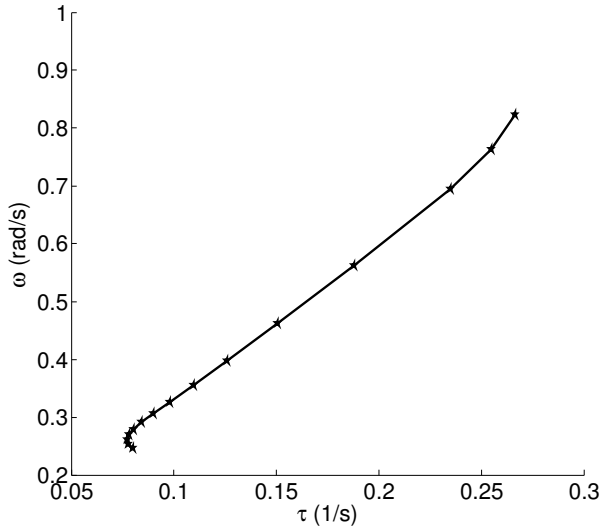

(c) Phugoid oscillation

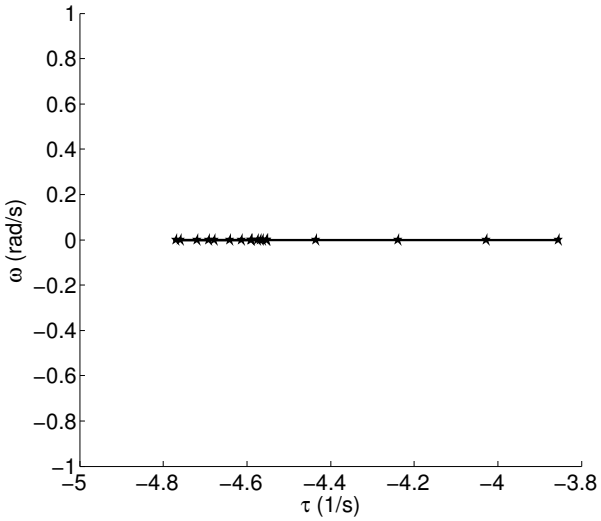

(d) Aperiodic pitch mode 1

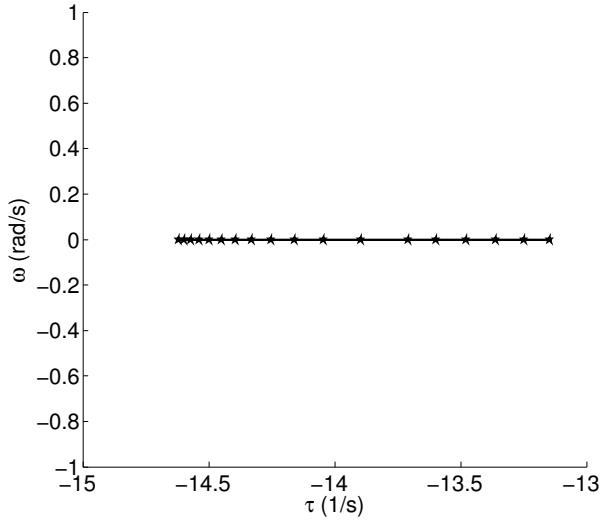

(e) Roll mode

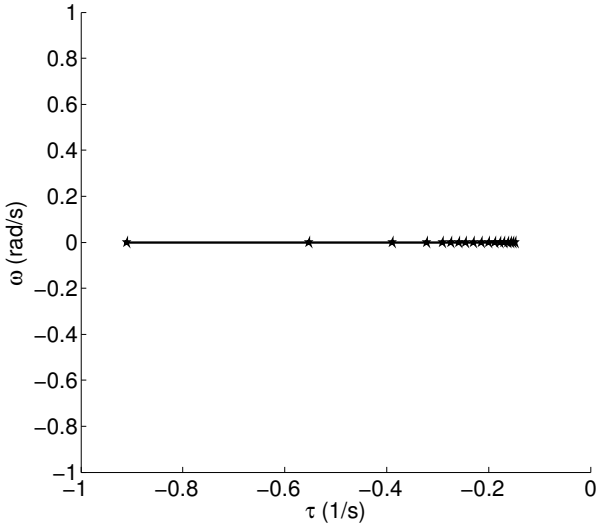

(f) Spiral mode

Fig. 5. Loci of the BO 105 eigenvalues as a function of forward speed for baseline radius and chord

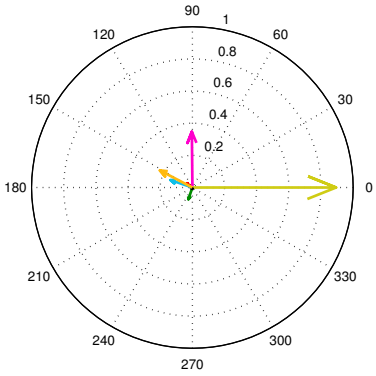

(a) Dutch roll oscillation, eigenvalue(-0.497 + i3.26)

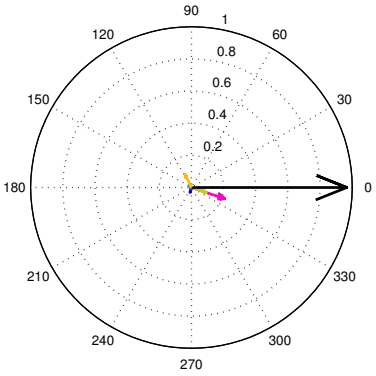

(b) Phugoid oscillation, eigenvalue(0.087 + i0.3)

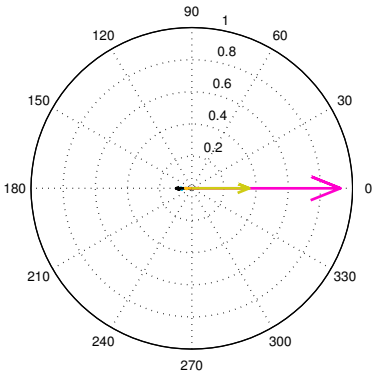

(c) Aperiodic pitch mode-1, eigenvalue(-4.60)

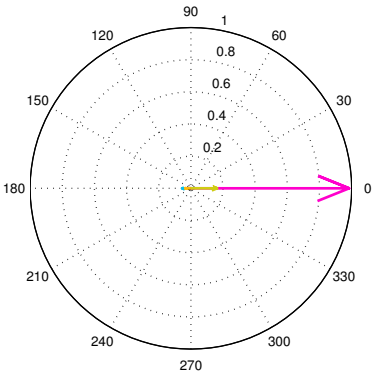

(d) Aperiodic pitch mode-2, eigenvalue(-2.02)

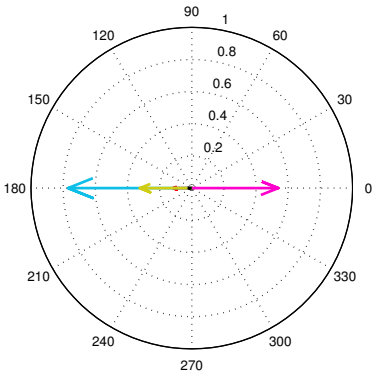

(e) Roll mode, eigenvalue(-14.42)

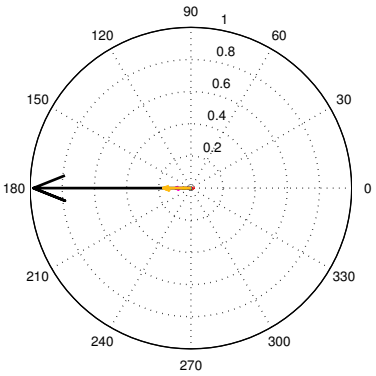

(f) Spiral mode, eigenvalue(-0.183)

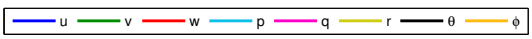

Fig. 6. BO 105 eigenvectors at forward speed of 148.16 km/hr (80 knots) for baseline radius and chord

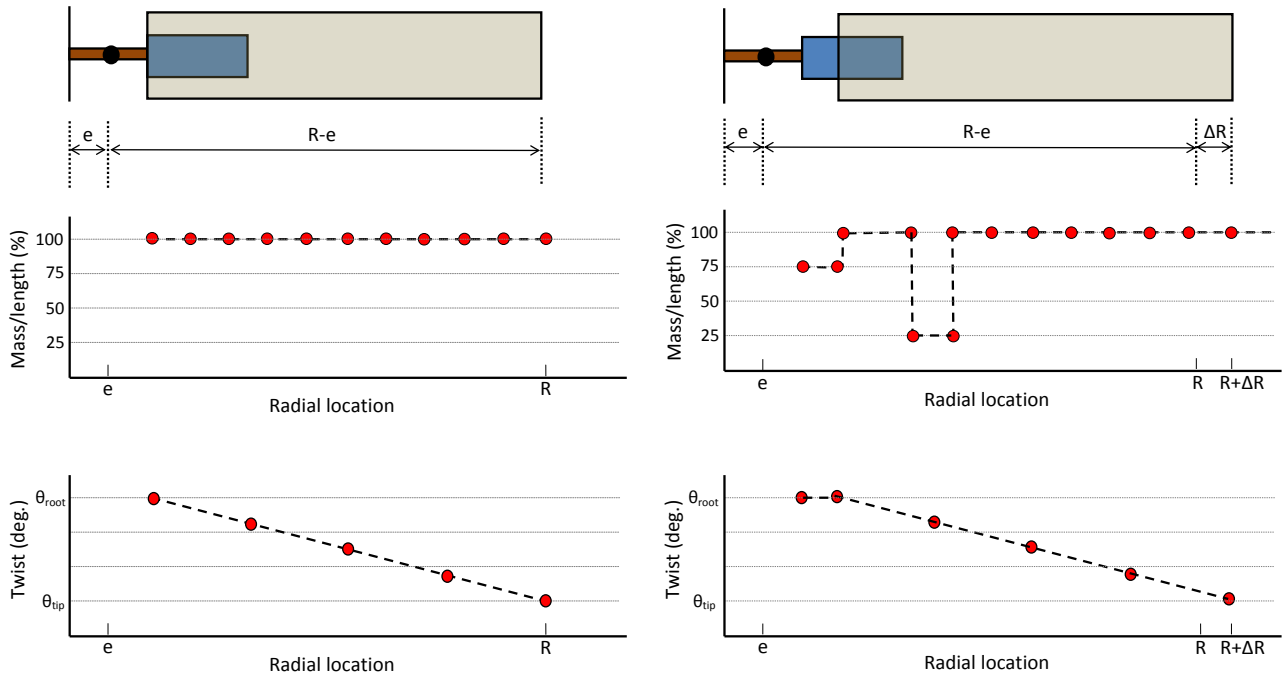

(a) Baseline blade model

(b) Variable radius blade model

Fig. 7. Variation of mass/length and blade twist with radial location for variable radius blade

more stable compared to 105% radius. The rotor with 110% radius is the least stable at low speeds. A significant variation in dutch roll mode occurs between the speeds of 39.24 km/hr to 141.26 km/hr where baseline radius is more stable and 110% radius is least stable. Beyond 141.26 km/hr, 110% radius becomes the most stable configuration for dutch roll and baseline radius becomes the least stable. Variation of phugoid mode oscillation with radius change is shown in the Fig. 8(d). The stability and the frequency of the phugoid mode decreases with increase in radius.

Figure 9 shows the coupling of the pitch mode-1 and pitch mode-2 for the case of 105% and 110% radius. The frequency of the coupled pitch mode increases with forward speed as its stability remains almost constant. The stability of the coupled pitch decreases with increase in blade radius. For the case of 110% radius, the inception of the coupled mode starts at the speed of 120.85 km/hr as shown in Fig. 10(c). The yaw rate (r) component becomes imaginary and has a phase angle of 342^o in the corresponding coupled pitch eigenvector. Fig. 10(a) and 10(b) shows the absence of coupling in the pitch mode at the speed of 120.85 km/hr.

The pitch mode coupling for 105% radius starts at a speed of 148.32 km/hr. Figures 11(b) and 11(c) show that the yaw rate (r) component of the pitch mode eigenvector has a phase angle of 350^o and 334^o for 105% and 110% radius respectively. The absence of coupling in the pitch mode for the baseline radius can be observed from Fig. 11(a).

Effect of Variation of Chord Length

The chord length of the blade is increased by 10% and 20% of the baseline and its effect on the stability modes are observed. The roll mode variation due to chord length is shown in the Fig. 12(a). The stability of the roll mode decreases with increase in chord length. The stability of the spiral mode slightly decreases with increase in chord length at higher speeds as shown in the Fig. 12(b). The stability of the spiral mode doesn't show any considerable change at low speed with change in chord length.

Dutch roll mode oscillation variation with chord length shows an analogous variation as that of the radial length increase of the blade as seen in the Fig. 12(c). The stability of the dutch roll mode decreases with increase in chord length up to a speed of 141 km/hr. Further increase in forward speed shows the reversal of the trend observed at lower speeds for the stability of the dutch roll mode, where the baseline becomes more stable than the cases with increased chord length. Fig. 12(d) shows the variation of phugoid oscillation with chord length. Both the stability and frequency of the phugoid mode decreases with increase in forward speed.

The pitch mode-1 and pitch mode-2 couples as the chord length is increased from the baseline value as seen from the Fig. 13. The stability of the coupled pitch mode decreases with increase in chord, however the frequency of the coupled pitch mode increases with increase in chord length.

CONCLUSIONS

This paper studies the effect of variable geometry blade shape on the helicopter stability. First a 6 DoF flight dynamics model is developed and validated with simulated and experimental data from available literature. For this rotor dynamics model using rigid flap degree of freedom is developed and coupled to a quasi-steady aerodynamics model equipped with

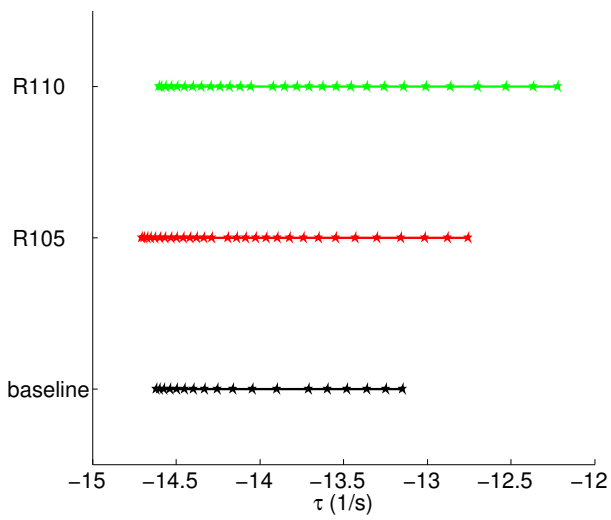

(a) Roll mode variation with radius

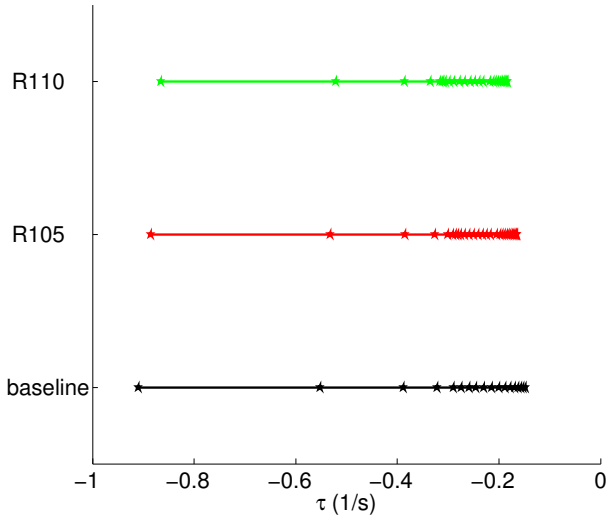

(b) Spiral mode variation with radius

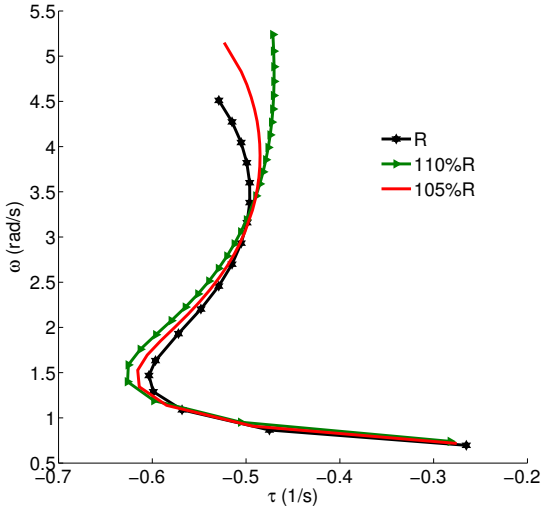

(c) Dutch roll oscillation variation with radius

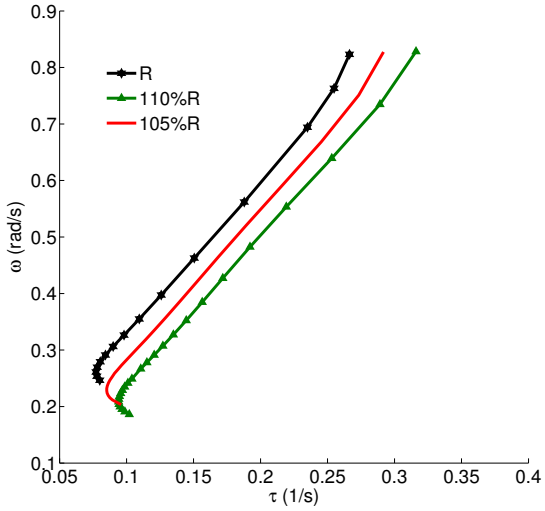

(d) Phugoid mode variation with radius

Fig. 8. Variation of eigenvalues with radius

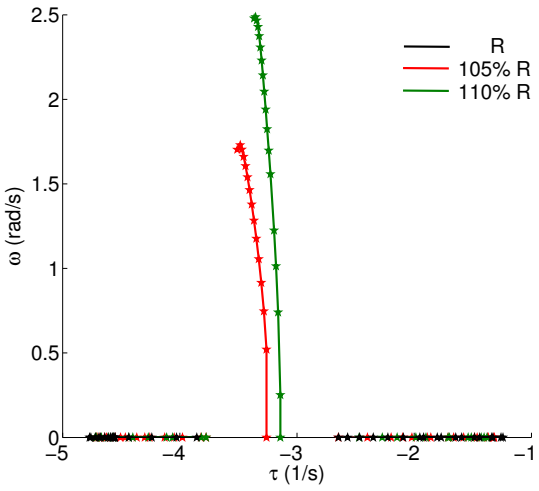

Fig. 9. Coupling of pitch modes for radius variation

non-uniform Drees inflow model. The DLR research Bo105-S123 helicopter is chosen for the baseline study. Some of the key conclusions drawn from the present study are listed below:

1. The stability of the roll mode decreases with increase in blade radial length at low speeds and it is comparatively insensitive to the radius change at high speeds. Blade chord length increase decreases the stability of the roll mode uniformly during low as well as high speeds.

2. The stability of the spiral mode at higher speeds increases with increase in radius and chord. At lower speeds, change of radius and chord has less significant impact on the spiral model stability.

3. Oscillatory Dutch roll mode shows a decrease in stability with increase in radius up to a forward speed of 141.26 km/hr. Further increase in forward speed increases the stability with increase in blade radius. Dutch roll oscillations also shows similar trend with chord length increase.

4. The stability and frequency of the phugoid mode decreases with increase in both radius and chord.

5. The increase in the radius or chord from the baseline value results in appearance of a new coupled pitch oscillatory mode which is formed due to the merging of aperiodic pitch mode-1 and aperiodic pitch mode-2.

6. The present computational model shows fair correlation with the flight test data for both trim and stability analysis of BO 105.

REFERENCES

[1]Frandenburgh, E. A., Murill, R. J., Kiely, E. F.," Dynamic Model Wind Tunnel Tests of a Variable-Diameter, Telescoping Blade Rotor System (TRAC ROTOR),"Sikorsky Aircraft, USAAMRDL-TR-73-32, Eustis Directorate, U.S. Army Air Mobility Research and Development Laboratory, Fort Eustis, VA, AD-771 037, July 1973.

[2]Matuska, D., Dale, A., Lorber, P.,"Wind Tunnel Test of a Variable-Diameter Tiltrotor (VDTR) Model,"NASA Contractor report 177629, Ames Research Center, NAS2-13484, January 1994.

[3]Migliore, P. G., Quandt, G. A., and Miller, L. S.,"Wind turbine trailing edge aerodynamic brakes,"Technical Report NREL/TP-441-7805, NREL, April 1995.

[4]Marrant, B. A. H., and Van Holten, T. H.,"Comparison of Smart Rotor Blade Concepts for Large Offshore Wind Turbines,"Off shore wind energy and other renewable energies in Mediterranean and European Seas Proceedings, Rome, Italy, September 5–7, 2012.

[5]Moser, P., Barbarino, S. and Gandhi, F., "Helicopter Rotor-Blade Chord Extension Morphing Using a Centrifugally Actuated Von Mises Truss," *Journal of Aircraft*, Vol. 51, (5), 2014, pp. 1422–1431.

[6]Khoshlahjeh, M. and Gandhi, F., "Extendable Chord Rotors for Helicopter Envelope Expansion and Performance Improvement," Journal of the American Helicopter Society, Vol. 59, (1), pp.1–10.

[7]Kang, H., Saber, H. and Gandhi, F., "Dynamic Blade Shape for Improved Helicopter Rotor Performance," *Journal of the American Helicopter Society*, Vol. 55, (3), 2010, pp. 32008-1–32008-11.

[8]Mistry, M. and Gandhi, F., "Helicopter Performance Improvement with Variable Rotor Radius and RPM," *Journal of the American Helicopter Society*, Vol. 59, (4), October 2014, pp. 17–35

[9]Leishman, J. G., "Principles of Helicopter Aerodynamics," 2nd ed., Cambridge University Press, New York, NY, 2006.

[10]Padfield, G.D., "Helicopter Flight Dynamics," 2nd ed., Blackwell Publishing, 2007.

[11]Kaletka, J., Gruenhagen W. V., Tischler M. B. and Fletcher J. W., "Time and FrequencyDomain Identification and Verification of BO 105 Dynamic Models," *Journal of the American Helicopter Society*, Vol. 36, (4), October 1991, pp. 25–38

[12]AGARD, "Rotorcraft System Identification," AGARD Advisory Report AR 280,1991

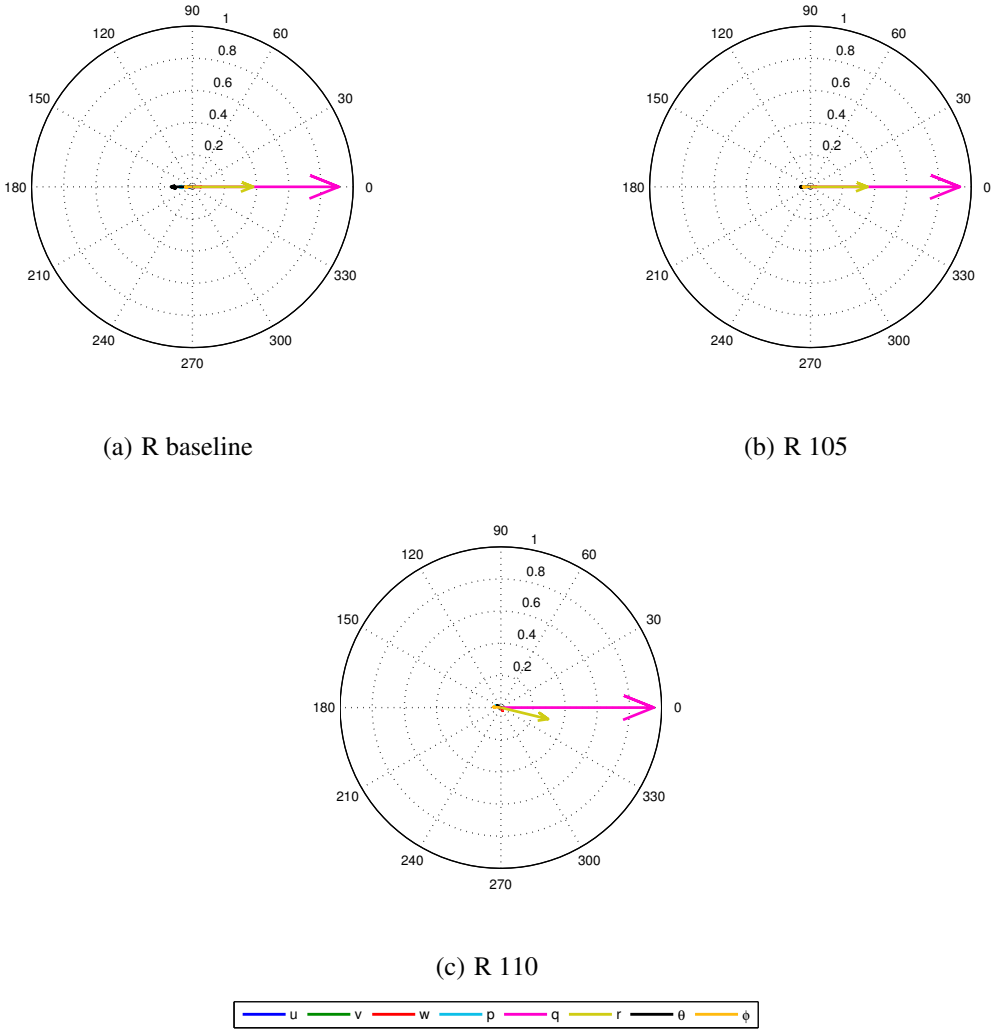

(a) R baseline

(b) R 105

(c) R 110

Fig. 10. Eigenvector at 120.85 Km/h for pitch mode-1 and pitch mode-2 corresponding to various radial length

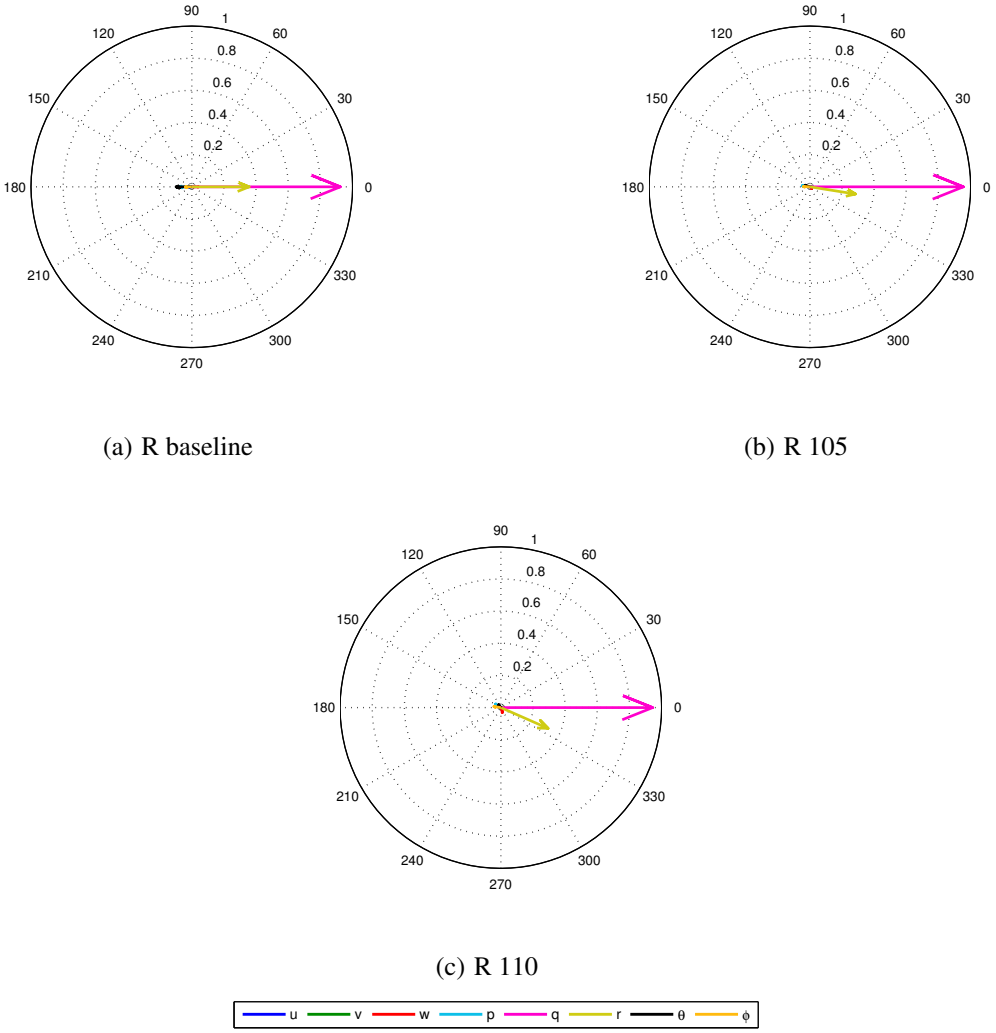

(a) R baseline

(b) R 105

(c) R 110

Fig. 11. Eigenvector at 148.32 Km/h for pitch mode-1 and pitch mode-2 corresponding to various radial length

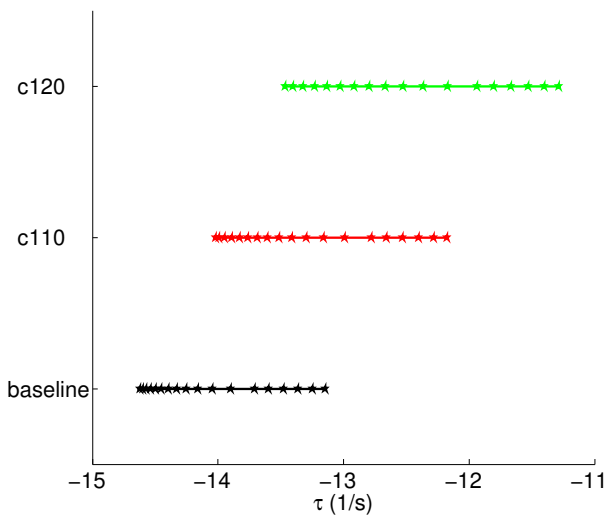

(a) Roll mode

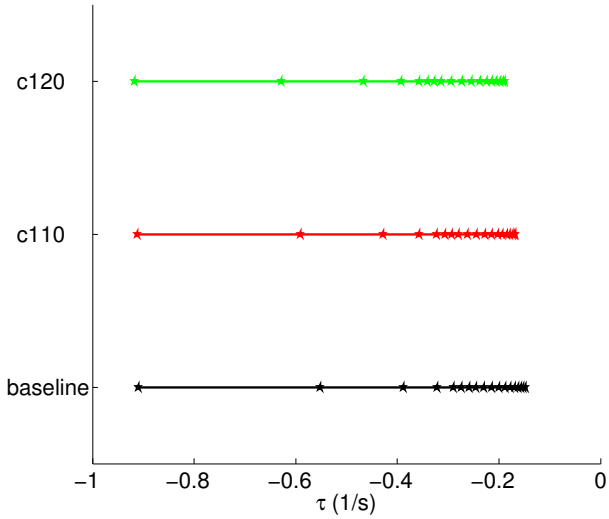

(b) Spiral mode

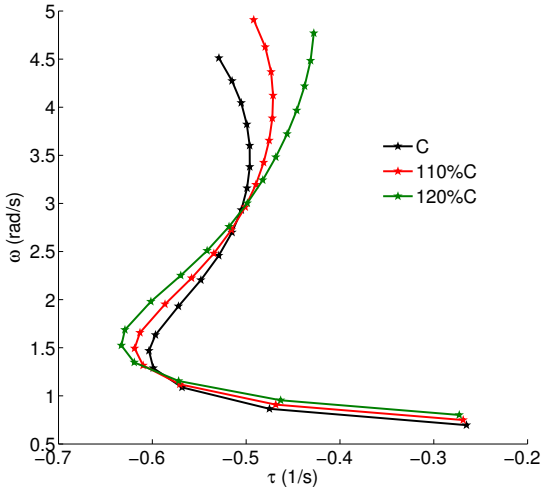

(c) Dutch roll oscillation

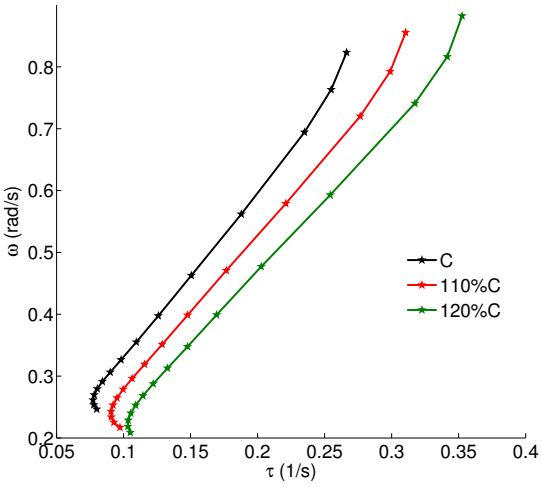

(d) Phugoid oscillation

Fig. 12. Variation of the loci of eigenvalues with chord

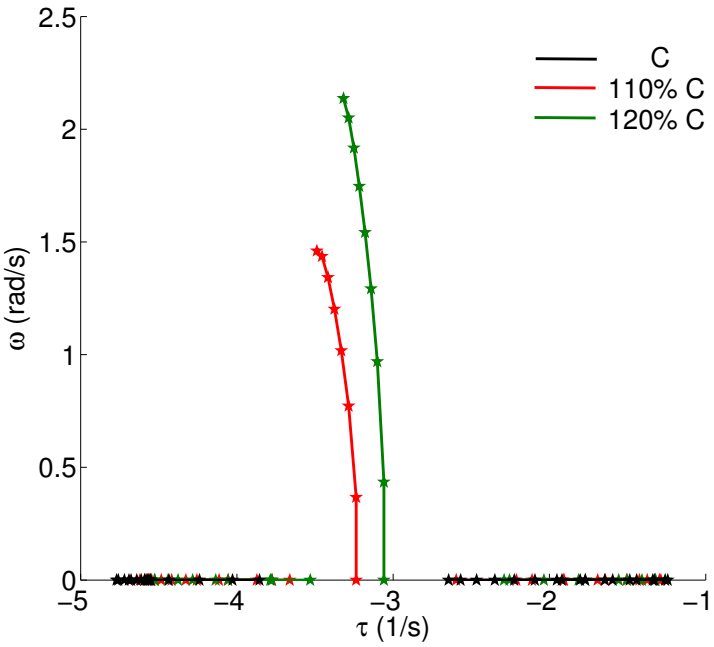

Fig. 13. Coupling of pitch modes for chord variation